Ab Initio Computer Simulation of the Early Stages of Crystallization: Application to $Ge_2Sb_2Te_5$ Phase-Change Materials

T. H. Lee and S. R. Elliott

Department of Chemistry, University of Cambridge, Lensfield Road, Cambridge CB2 1EW, United Kingdom

(Received 12 April 2011; revised manuscript received 30 July 2011; published 27 September 2011)

By virtue of the ultrashort phase-transition time of phase-change memory materials, e.g., $Ge_2Sb_2Te_5$, we successfully reproduce the early stages of crystallization in such a material using *ab initio* molecular-dynamics simulations. A stochastic distribution in the crystallization onset time is found, as generally assumed in classical nucleation theory. The critical crystal nucleus is estimated to comprise 5–10 $(Ge, Sb)_4Te_4$ cubes. Simulated growth rates of crystalline clusters in amorphous $Ge_2Sb_2Te_5$ are consistent with extrapolated experimental measurements. The formation of ordered planar structures in the amorphous phase plays a critical role in lowering the interfacial energy between crystalline clusters and the amorphous phase, which explains why Ge-Sb-Te materials exhibit ultrafast crystallization.

DOI: 10.1103/PhysRevLett.107.145702 PACS numbers: 64.60.Cn, 61.43.Bn, 61.43.Dq

The crystallization of amorphous materials has been extensively explored due to its scientific and technological importance. The crystallization process can be more readily observed in glasses than in liquids since the former generally involves longer times, which enables one to verify classical nucleation theory (CNT) by direct quantitative experimental measurements [1]. The slower crystallization in glasses is mostly due to the lower diffusivity of atoms and the higher interfacial energy.

On the other hand, phase-change (PC) memory materials, such as $Ge_2Sb_2Te_5$ (GST), show extraordinarily fast crystallization (of the order of nanoseconds) under optical or electrical pulse excitation. This property is a key reason for their usability in optical data-storage media or nonvolatile electronic memory devices [2,3].

Understanding of crystallization in glasses is lacking because of incomplete knowledge of the microscopic structural changes during nucleation and growth. Notably, the initial structure of new crystal phases, or the structure of the interface between crystalline clusters and the parent amorphous phase, is still unknown [1].

X-ray diffraction, or even high-resolution transmission electron microscopy, is unable to reveal ordered structures of a few nanometers in size embedded in an amorphous matrix [4], preventing one from observing the early stages of the phase-transition process. Although the existence of subcritical crystal nuclei in the amorphous state of PC materials has been reported using fluctuation electron microscopy, this technique could not provide detailed information on the atomic structure [5].

Ab initio molecular-dynamics (AIMD) simulations based on density functional theory are a powerful tool in understanding the atomic structure of materials [6]. However, the substantial computational times required to simulate PC processes generally inhibits its use for this purpose. Thus, most research on PC materials has investigated structural or electronic properties of the initial amorphous or final crystalline products of the phase transition, and inferred possible mechanisms for fast crystallization from a comparison between the amorphous and crystalline structures [7–9].

Here, we describe AIMD simulations of the amorphous-to-crystalline phase transition in GST materials, known to show extraordinarily fast crystallization speeds. The simulations were performed with total simulation times (~ 0.5 ns) close to the experimental time scale. The results, obtained for larger models than in our previous work [10], show all the essential details of how atoms in amorphous GST organize structurally and chemically on thermal annealing, leading to crystallization. The simulated atomic dynamics reveal that the mechanism of the fast phase transition of GST materials is closely associated with the formation of chemically correct, medium-range ordered (planar) structures driven by the intrinsic electronic structure of the atoms and their bonding properties, which facilitates nucleation and growth.

We have performed AIMD simulations of GST at constant volume (to simulate capped films) using the Vienna *ab initio* simulation package (VASP) code [11,12]. Three 180-atom models (1, 2, 3), with a density (6.11 g/cm^3) intermediate between the amorphous and crystalline densities, were independently quenched to 300 K from a liquid at 1073 K with a quench rate of -15 K/ps to form glasses [and having initial internal pressures of $\sim$1.2 (1, 2) and $\sim$1.6 GPa (3)]. In addition, one of these models (4) was relaxed to the amorphous-phase density of 5.88 g/cm^3 (resulting in an internal pressure of 0.57 GPa at 300 K), and another (5) was relaxed to a density of 5.66 g/cm^3, corresponding to an initially near-zero pressure (25 MPa) at 300 K. All these models were then crystallized by annealing at a temperature (600 K) intermediate between the glass-transition and melting temperatures. During the annealing runs, the internal pressures rose slightly to 1.4 (1, 2), 0.9 (4) and 0.4 GPa (5), respectively. The latter

pressure is comparable to the maximum pressure found experimentally in capped layers of GST on crystallization due to the density difference between amorphous and crystal phases [13]. Moreover, these pressures are well below that (~ 15 GPa) at which amorphization starts to occur in fcc GST [14]. During annealing, the same gradual self-organization of atoms occurs in all models, forming an ordered seed in the amorphous phase, with subsequent growth into a crystalline phase on annealing, best characterized in terms of the evolution of structural units constituting the crystalline phase [see Figs. 1(a)–1(d)].

The smallest structural element in the metastable rocksalt phase of crystalline GST [15] is a fourfold ring. Connected parallel fourfold rings form another (medium-range) structural unit, a plane. The most symmetric structural unit is a cube consisting of six connected fourfold rings. The ideal rocksalt structure comprises cubes sharing all faces with six other cubes, or, equivalently, perpendicularly cross-linked planes of fourfold rings.

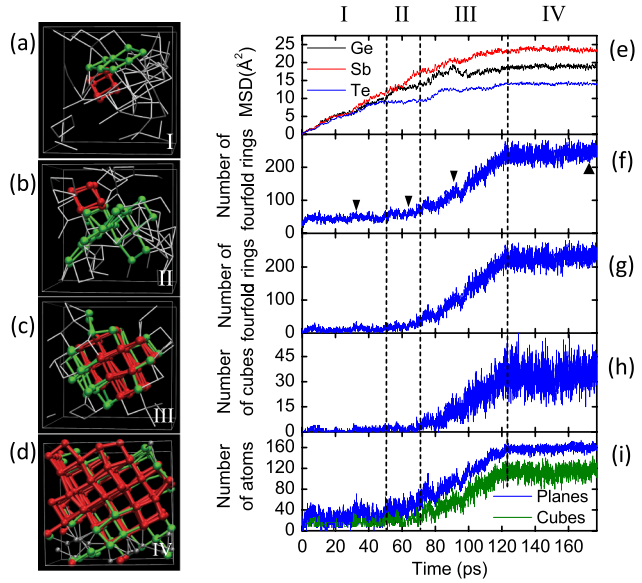

FIG. 1 (color online). Atomic configurations (model 1) during the crystallization process in amorphous $Ge_2Sb_2Te_5$ and the evolution of structural units on annealing at 600 K. (a)–(d) Snapshots of model configurations at different stages of crystallization, periods I–IV (see text). The arrows in (f) indicate the times at which these snapshots were taken. (a) Formation of structural units during the incubation period I. A significant number of fourfold rings (silver) exist, but only a few planes (green) or cubes (red) are formed occasionally. (b) Development of ordered layer structures at the crystallization site. (c) A cube cluster and planes extending from the cluster interface. (d) Completely crystallized phase with a crystal-glass interface. (e) Mean-squared displacement (MSD) for each type of atom. (f)–(i) Evolution of structural units: (f) fourfold rings; (g) number of fourfold rings forming planes; (h) number of cubes; (i) number of atoms forming planes or cubes.

A signature of the onset of crystallization is the point at which the number of cubes forming a structurally ordered cluster starts to increase. On this definition, crystallization started in this simulation at about 70 ps, being completed at 120 ps [Fig. 1(h)]. We denote this time period as III. The time up to period III is therefore an incubation period for the crystallization. Period IV represents a completely crystallized state.

During the incubation period I, a certain number of fourfold rings always exists in the amorphous phase [Figs. 1(a) and 1(f)]. A small proportion of these also forms transient discrete planes or cubes, with random orientations, via repeated formation and annihilation, due to thermal fluctuations [Figs. 1(g) and 1(h)]. After the formation of fluctuating structural units or their clusters, a medium-range ordered planar structure is generated at the crystallization site in period II [Figs. 1(b), 1(g), and 1(i)]: a cluster of planes consisting of more than two parallel fourfold rings develops near the center of a crystallization site at the expense of either discrete or connected (but nonparallel) fourfold rings [Fig. 1(b)] [12]. As annealing proceeds, a cluster of cubes forms within this planar structure, then grows rather than decays [Figs. 1(c) and 1(h)]. At the beginning of period III (before an almost linear growth of the cluster), there is a period in which a clustered group of cubes maintains its configuration for about 10 ps [Fig. 1(h)] [12]. Such a cluster of cubes grows as atoms adhere to its interface, forming first a shell of planes (i.e., fourfold rings connected with the same bond-orientational order), and then cubes [Figs. 1(c) and 1(i)]. Figure 1(d) shows the final configuration, which consists of a crystalline phase (rocksalt structure without any internal vacancies) and the crystal-glass interface. The same behavior was observed for all models, irrespective of density or internal pressures. Te atoms in the crystalline phase form a perfect fcc sublattice of the rocksalt structure, while Ge or Sb atoms occupy sites in the other sublattice (being slightly Ge rich). At the crystal-glass interface, the structure is more disordered, and a high concentration of homobonds, especially Te-Te and Sb-Sb, exists, along with a significant number of vacancies.

Most cubes form and grow from the center of the crystallization site; Fig. 1(h) shows the growth of such entities. The shape of the ordered cubic structures is not spherical, but rather ellipsoidal [16], so we calculated their effective radii from the total volume of cubes forming that structure. The time evolution of the crystal-cluster radius computed in this way for models 1–3 is shown in Fig. 2. These amorphous models showed a stochastic distribution in the onset times of crystallization (end of region II) (i.e., 70, 190, and 270 ps), as observed in experiments and assumed in CNT [1,5]. In period III, there is an almost linear growth of the cluster radius with time.

The experimental growth rate of GST at 600 K was estimated, based on data reported by Kalb *et. al.* [17];

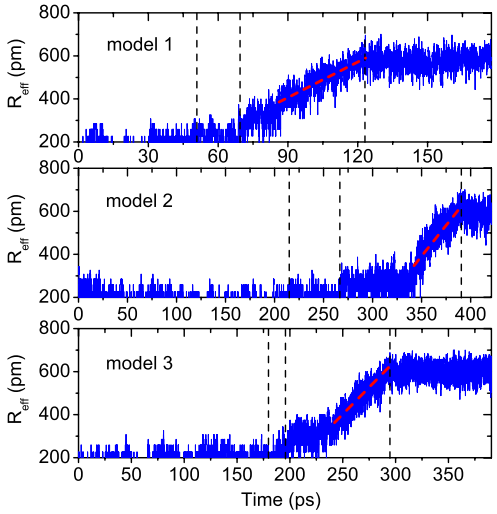

FIG. 2 (color online). Time evolution of the effective radius (R_{eff}) of the cube cluster for models 1–3. Dashed red lines are linear fits for the growth velocity. The vertical dotted lines indicate the periods I–IV, as in Fig. 1.

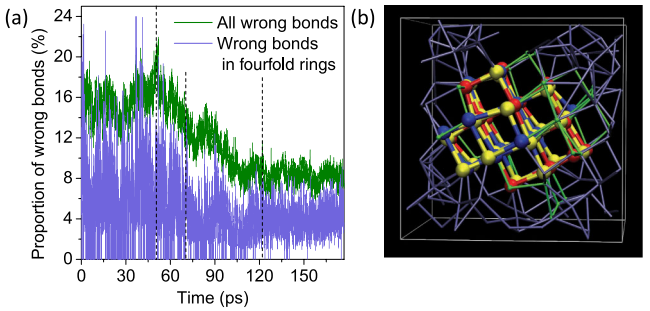

FIG. 3 (color online). Chemical ordering during crystallization (model 1). (a) Proportion of wrong bonds on average and in fourfold rings. The large fluctuations in period I indicate that the discrete fourfold rings are relatively unstable compared to the fourfold rings comprising planes or cubes. (b) Model configuration showing a cube cluster with perfect chemical ordering. Ge (blue) and Sb (red) atoms are coordinated by Te (yellow) atoms in the cluster. Atoms in planes (green) lie at the interface between the cluster and the amorphous phase (purple).

they found that the crystal-growth velocities, u (pm/s), satisfied the Arrhenius relation and they obtained an activation energy of 2.35 ± 0.05 eV for crystal growth in GST. The logarithm of u extrapolated to 600 K from their empirical Arrhenius relation has values in the range 24–29. This corresponds well to our simulated crystal-growth results for ln u of 29.34, 29.36, 29.17, 29.28 and 28.73 ± 0.01 for models 1–5, respectively (see Fig. 2). To the best of our knowledge, this is the first time that AIMD simulations have reproduced quantitatively an experimental (extrapolated) crystal-growth rate.

It is interesting to consider the correspondence between our simulation results and CNT. In CNT, once a cluster greater than critical size is generated by fluctuations, it can grow. Of the nucleation process preceding growth, very little is observable directly; no experiment has directly measured the size of the critical nucleus, except in colloidal crystallization [16]. According to our simulations [12], once the size of clusters becomes larger than a certain volume (corresponding to approximately 5–10 connected cubes), they successfully start to grow, rather than decay, in the period III, following the incubation period. Thus, our simulations indicate that a cluster of this size behaves as the critical-nucleus size for GST at 600 K. If this cluster, solely of connected cubes, corresponds to the actual critical-nucleus size, the interfacial energy between the metastable rocksalt phase of GST and the amorphous phase, calculated from CNT, is ~ 5 mJ/m^2, that is approximately an order of magnitude smaller than that between the hexagonal and liquid phases of GST [40 ± 3 mJ/m^2] [12,18]. However, if the region of quasiordered planes around such clusters is also included in the estimation of the critical-nucleus size, the size is correspondingly larger, and hence the interfacial energy is also larger. Moreover, the nonlinear ensemble-averaged growth rate (i.e., dependent on the cluster size), predicted by CNT [19], is not clearly revealed in our simulations. The absence of a nonlinear-growth stage in our simulations may be related to the system size. However, it is known that CNT is inaccurate for very small crystal nuclei [19], as found in these simulations; this may also be the cause of this discrepancy. Further studies are needed to clarify this issue.

Another important characteristic of the phase transformation in GST found in this study is chemical ordering: Ge and Sb atoms prefer to be coordinated by Te atoms, and vice versa. The general trend of chemical ordering is shown in Fig. 3(a). The proportion of wrong bonds, i.e., Te-Te, Ge-Ge, Sb-Sb, and Ge-Sb [Fig. 3(a)], calculated with a cutoff distance of 3.2 Å, started to decrease during crystallization (periods II and III) and then stabilized after crystallization was complete (period IV) [10]. The wrong bonds remaining in region IV are mostly homobonds at the crystal-glass interface; almost perfect chemical ordering is observed in the crystalline phase [Fig. 3(b)]. In addition, as shown in Fig. 3(a), it is clear that, in general, a higher degree of chemical ordering is manifested in fourfold rings throughout the annealing process. The percentage of wrong neighbors in cubes, as well as in planes, is even lower than in isolated fourfold rings [12]. Therefore, the gradual transformation to fourfold rings, and then to planes or cubes, during crystallization gradually reduces the proportion of wrong bonds. Thus, structural ordering is always accompanied by chemical ordering.

The most significant features found during the crystallization process in all simulations are (i) the formation of a cluster of cubes of atoms in the region of an ordered planar structure, and (ii) the growth of that cluster, preceded by growth of a layer of planes at the interface

[see Fig. 1(i)]. Such behavior was not observed for transient structural units in the incubation period I. It can be speculated that the interfacial energy between the crystal cluster and the surrounding amorphous phase is significantly reduced due to the presence of the shell of planes (having the same bond orientation as that of the cluster of cubes) at the interface, thereby facilitating crystallization. The interfacial energy between the metastable rocksalt and amorphous phases of GST is also expected to be anomalously small because of the very similar (defective) octahedral atomic coordination in both solid phases of this material, consistent with the low interfacial energy described previously. It should be emphasized that, in GST, this is possible because the average bond angles are all $\sim 90°$, which facilitates the formation of the intermediate structure (i.e., planes of fourfold rings). Similar preferential crystallization in regions of high structural order has been observed in Brownian dynamic simulations of colloidal liquids [20]. Furthermore, a similarly small interfacial energy has been observed in a Zr-based metallic glass where the quasicrystal and glass have similar icosahedral ordering [21].

An important consequence is that the highest crystallization speed to the rocksalt structure can be anticipated when all atoms have bonding configurations with a 90° bond angle, as in pure p bonding. Indeed, most PC materials have a distorted rocksalt (cubic) structure as a metastable crystalline phase with such a bonding character [22], which, in turn, suggests that lowering the interfacial energy by forming a planar structure prior to the formation of a more symmetric cubic structure might be a general characteristic of fast PC materials. On the other hand, other atomic and electronic configurations, such as tetrahedral coordination involving sp^3 hybridization, can present an energy barrier for the amorphous-crystal phase transition, so the presence of these configurations may be beneficial for the room-temperature stability of the amorphous phase. Sb and Te atoms have valence-electron configurations of $5s^2 5p^3$ and $5s^2 5p^4$, respectively, allowing pure p bonding. However, Ge atoms have a $4s^2 4p^2$ configuration and often undergo sp^3 hybridization in the amorphous state [23], resulting in tetrahedral bonding and 109° bond angles, as found in our simulations. Recently, it was reported that Ge atoms may also adopt a pure p-bonding-like, threefold coordinated configuration, without a large penalty in energy, by accepting lone-pair electrons donated by Te atoms [24]. Such configurations are also reproduced in our simulations [12]. It was also found that almost all Ge atoms had 90° bond angles during annealing of the amorphous phase [12]. Therefore, we argue that fast phase transitions are possible in GST materials because thermal energy enables Ge atoms to overcome the energy barrier between sp^3 and pure p-bonding-like configurations, transforming most Ge atoms to the latter configuration. The existence of multiple-valence-electron configurations for Ge atoms without a large penalty in energy may be why, paradoxically, GST materials are stable in the amorphous state at room temperature but also exhibit ultrarapid crystallization on thermal annealing.

In conclusion, we have simulated the formation and growth of crystalline clusters in amorphous GST on thermal annealing using AIMD. The simulations confirmed the stochastic character of the onset of crystallization, as assumed in CNT, and the growth rate of crystalline clusters matches the experimentally extrapolated crystal-growth rate. Moreover, our simulations revealed that crystallization is facilitated by the similar local defective octahedral coordination in crystalline and parent amorphous phases. This similarity is due to the p-type bonding character commonly found in atoms constituting GST materials. The formation of (chemically correct) medium-range ordered planar structures is promoted by this bonding configuration, which may lower the interfacial energy and lead to the ultrafast crystallization speed.

We thank A. L. Greer for critical comments on the manuscript. Financial support by the Engineering and Physical Sciences Research Council (United Kingdom) is gratefully acknowledged. AIMD simulations were performed using the Cambridge High-Performance Computer Facility.

[1] K. F. Kelton and A. L. Greer, *Nucleation in Condensed Matter: Applications in Materials and Biology* (Elsevier, Oxford, 2010), pp. 279–329.
[2] M. Wuttig and N. Yamada, Nature Mater. **6**, 824 (2007).
[3] N. Yamada *et al.*, J. Appl. Phys. **69**, 2849 (1991).
[4] M. M. J. Treacy *et al.*, Rep. Prog. Phys. **68**, 2899 (2005).
[5] B.-S. Lee *et al.*, Science **326**, 980 (2009).
[6] R. M. Martin, *Electronic Structure: Basic Theory and Practical Methods* (Cambridge University Press, Cambridge, 2004).
[7] J. Akola and R. O. Jones, Phys. Rev. B **76**, 235201 (2007).
[8] P. Jóvári *et al.*, Phys. Rev. B **77**, 035202 (2008).
[9] M. Krbal *et al.*, Phys. Rev. B **83**, 054203 (2011).
[10] J. Hegedüs and S. R. Elliott, Nature Mater. **7**, 399 (2008).
[11] G. Kresse and J. Hafner, Phys. Rev. B **47**, 558 (1993).
[12] See Supplemental Material at http://link.aps.org/supplemental/10.1103/PhysRevLett.107.145702 for full details of computational methods and supporting results.
[13] Q. Guo *et al.*, Appl. Phys. Lett. **93**, 221907 (2008).
[14] S. Caravati *et al.*, Phys. Rev. Lett. **102**, 205502 (2009).
[15] N. Yamada and T. Matsunaga, J. Appl. Phys. **88**, 7020 (2000).
[16] U. Gasser *et al.*, Science **292**, 258 (2001).
[17] J. Kalb, F. Spaepen, and M. Wuttig, Appl. Phys. Lett. **84**, 5240 (2004).
[18] J. A. Kalb, F. Spaepen, and M. Wuttig, J. Appl. Phys. **98**, 054910 (2005).
[19] K. F. Kelton and A. L. Greer, J. Non-Cryst. Solids **79**, 295 (1986).

[20] T. Kawasaki and H. Tanaka, Proc. Natl. Acad. Sci. U.S.A. **107**, 14036 (2010).
[21] Y. T. Shen, T. H. Kim, A. K. Gangopadhyay, and K. F. Kelton, Phys. Rev. Lett. **102**, 057801 (2009).
[22] T. Matsunaga and N. Yamada, Jpn. J. Appl. Phys. **41**, 1674 (2002).
[23] N. F. Mott and E. A. Davis, *Electronic Processes in Non-Crystalline Materials* (Clarendon Press, Oxford, 1979).
[24] M. Xu, Y. Q. Cheng, H. W. Sheng, and E. Ma, Phys. Rev. Lett. **103**, 195502 (2009).